Compact Dual-Band Bandpass Filter with High Selectivity Using Stub-Loaded Stepped-Impedance Resonators

Zhonghua Zhang[1, *], Ming Xia[1], and Guanglin Li[2]

Abstract—A novel compact dual-band bandpass filter with wide stopband using stub-loaded stepped-impedance resonators is presented in this paper. The characteristics of the dual-mode resonator are investigated by using even/odd mode analysis. The center frequencies and bandwidths of the two passbands can be controlled by adjusting the geometric dimensions of the stub-loaded stepped-impedance resonators. Moreover, the filter has been implemented with five transmission zeros to improve the selectivity. A prototype of a dual-band bandpass filter centered at 3 and 4.35 GHz has been designed and fabricated. The measured bandwidths are 8.3 and 4.6%, and the corresponding insertion losses are 1.7 and 1.6 dB, respectively. A compact dual-band bandpass filter with sharp roll-off rate of 113.3/56.7/56.7/170 dB/GHz, wide stopband of 5.3 GHz, and isolation between two passbands of 25 dB is achieved. The measured results are in good agreement with the simulated ones.

1. INTRODUCTION

As a result of the rapid progress in wireless communication systems, dual-band bandpass filters have become more and more attractive as one of the most important components. To meet the demand, many researches have been performed, and various design methods have been presented [1–11]. In [2], a dual-band bandpass filter was achieved by a cascade connection of a bandpass filter and a bandstop filter, with the drawback of a large circuit size. In [3], dual-band bandpass filters using stub-loaded resonators with two coupling paths were proposed to control bandwidths. However, these designs are limited to lower order filters either inherently or because of their complicated configurations. In [4], a dual-band bandpass filter can also be realized by using LTCC techniques. Though the circuit sizes of filters are very small, expensive fabrication and complex design procedures are the key problematic issues in this approach. In [5–7], two sets of independent resonators with input/output ports were adopted to design a dual-band filter by using an embedded structure. Although the center frequency of two passbands can be individually controlled, the structure of the dual-band bandpass filter is relatively complex. In [8–11], dual-band bandpass filters were designed by utilizing stepped impedance resonators (SIRs), which means that two resonant frequencies can be controlled by the impedance ratio and electrical length of the two sections SIRs. Nevertheless, the resonant frequencies of SIRs are dependent on the physical structure and coupling coefficients, which complicate the filter design.

In this paper, a novel compact dual-band filter with high selectivity and wide stopband is proposed by utilizing the coupling of two dual-mode SIR resonators. Even- and odd-mode theory is applied to analyze the dual-band characteristics and equivalent circuits of the resonators. The passband frequencies can be conveniently tuned to the desired values by controlling the corresponding resonator dimensions. Furthermore, a new coupling structure is introduced to improve wide stopbands and high selectivity. For validation, a dual-band filter is designed and fabricated, and the measured results of the dual-band filter are in good agreement with the full-wave simulated ones.

[1] Department of Intelligent Manufacturing and Industrial Security, Chongqing Vocational Institute of Safety Technology, Chongqing 404020, China. [2] School of Engineering and Technology, Southwest University, Chongqing 400715, China.

2. ANALYSIS OF THE DUAL-MODE SIR RESONATOR

The dual-mode SIR resonance unit designed on a dielectric substrate with a thickness of $0.508\,\text{mm}$ and relative permittivity of 2.2 is shown in Figure 1. It consists of a stub-loaded stepped-impedance transmission line and a short-end stub, where (Y_1 and Y_2, L_1 and L_2) and ($2Y_3$, L_3) are characteristic admittances and lengths of the stub-loaded stepped-impedance transmission line and short-end stub, respectively. Due to the symmetric feature of the dual-mode SIR resonator, even- and odd-mode analysis method can be used to characterize it.
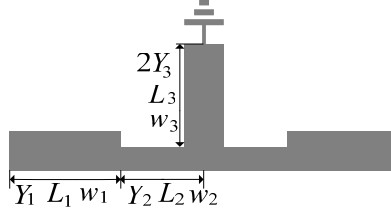
Figure 1. Dual-mode SIR resonator.

(a)   (b)
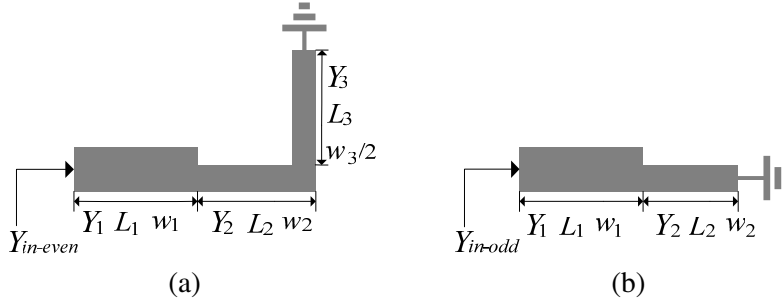
Figure 2. Equivalent circuits of dual-mode SIR resonator, (a) even-mode and (b) odd-mode.

When the even mode is excited, the symmetrical plane in Figure 1 is equivalent to a magnetic wall, and Figure 2(a) illustrates its equivalent circuit. Meanwhile, the odd mode is excited; the symmetrical plane can be modeled as an electric wall; its equivalent circuit is depicted in Figure 2(b). To obtain the resonant characteristics, we can analyze the input admittance and solve it by considering the resonant condition of $\text{Im}[Y_{\text{in}}] = 0$. Ignoring the influences of a step discontinuity, the input admittance $Y_{\text{in-even}}$ of the even-mode SIR, shown in Figure 2(a), is expressed as

$$Y_{\text{in-even}} = -jY_1 \frac{Y_2 - Y_1 \tan\theta_1 \tan(\theta_2 + \theta_3)}{Y_1 \tan(\theta_2 + \theta_3) + Y_2 \tan\theta_1} \tag{1}$$

where θ_1, θ_2, and θ_3 are the electrical lengths of the sections of lengths L_1, L_2, and L_3, respectively.

Similarly, the input admittance $Y_{\text{in-odd}}$ of the odd-mode SIR in Figure 2(b) can be extracted as

$$Y_{\text{in-odd}} = -jY_1 \frac{Y_2 - Y_1 \tan\theta_1 \tan\theta_2}{Y_1 \tan\theta_2 + Y_2 \tan\theta_1} \tag{2}$$

From the resonance condition $Y_{\text{in-even}} = 0$ and $Y_{\text{in-odd}} = 0$, the resonant frequencies can be expressed as

$$Y_2 - Y_1 \tan\theta_1 \tan(\theta_2 + \theta_3) = 0 \tag{3}$$

$$Y_2 - Y_1 \tan\theta_1 \tan\theta_2 = 0 \tag{4}$$

According to Equations (3) and (4), the even- and odd-mode resonant frequencies (f_{even} and f_{odd}) of the dual-mode SIR can be obtained as follows [12]

$$f_{\text{even}} \approx \frac{c}{4(L_1 + L_2 + L_3)\sqrt{\varepsilon_{\text{eff}}}} \tag{5}$$

$$f_{\text{odd}} \approx \frac{c}{4(L_1 + L_2)\sqrt{\varepsilon_{\text{eff}}}} \tag{6}$$

where c is the light speed in free space, and $\overline{\varepsilon_{eff}}$ is the dielectric constant defined as

$$\overline{\varepsilon_{eff}} = \frac{\varepsilon_r + 1}{2} + \frac{\varepsilon_r + 1}{2} \left[\left(1 + 12\frac{h}{\overline{w}} \right)^{-1/2} + 0.04 \left(1 - \frac{h}{\overline{w}} \right)^2 \right] \quad (7)$$

where $\overline{w}$ can be simply estimated as $\overline{w} = (w_1 + w_2)/2$, and ε_r and h denote the relative dielectric constant and thickness of the substrate, respectively.

Obviously, the resonance modes of the original resonator have been obtained as Equations (5) and (6). From the equations, we can observe that L_3 only affects f_{even}. Therefore, the dual-modes can be controlled. In order to verify the characteristics of the dual-mode SIR structure, the effects of the short-end stub and the stub-loaded stepped-impedance transmission line on the transmission responses are simulated, shown in Figure 3(a) and Figure 3(b), respectively. Figure 3(a) shows the transmission responses with scaling the length L_3 of the short-end stub, which states that the even-mode resonant frequencies are downward shift while the odd-mode resonant frequencies remain unchanged as L_3 is increased. In addition, the simulation results of resonator with different lengths L_1 of stub-loaded stepped-impedance transmission line are shown in Figure 3(b). It can be observed that the even- and odd-mode resonant frequencies are shifted to left-side when L_1 is increased from 3 to 5 mm (all the other dimensions remain unchanged). Thus, these conclusions are in accordance with the above analysis.
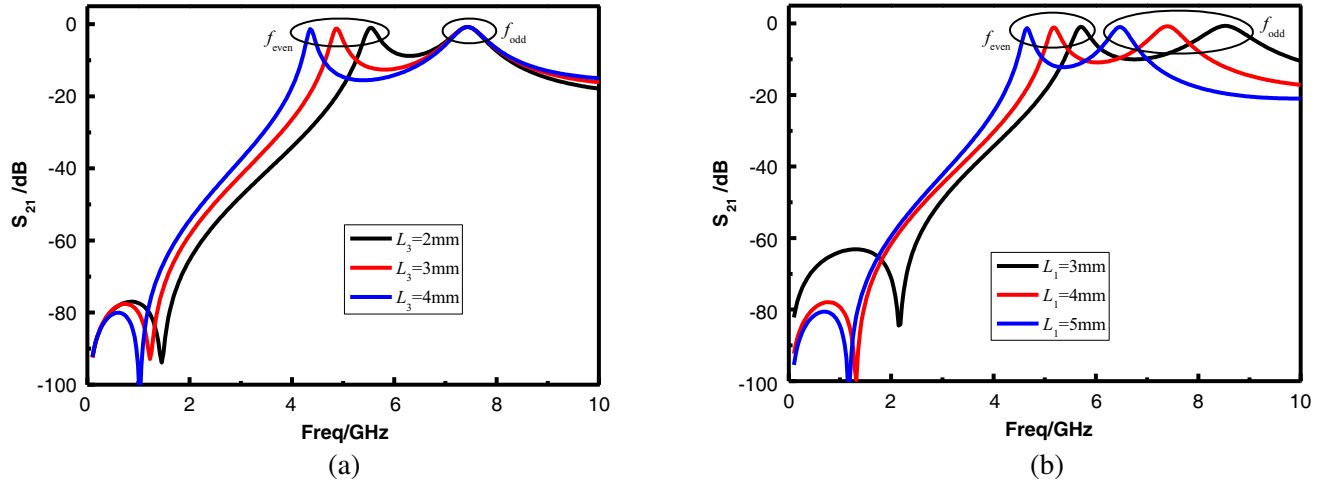
Figure 3. (a) The transmission responses of the dual-mode SIR resonance structure with different L_3 and (b) the transmission responses of the dual-mode SIR resonance structure with different L_1. The designed initial parameters are: $L_1 = 4\,\text{mm}$, $w_1 = 0.7\,\text{mm}$, $L_2 = 5\,\text{mm}$, $w_2 = 0.5\,\text{mm}$, $L_3 = 2.5\,\text{mm}$, $w_3 = 1\,\text{mm}$.

3. FILTER DESIGN

Based on the dual-mode SIR resonators, a dual-band bandpass filter is designed. The layout of the proposed filter is shown in Figure 4. It consists of two dual-mode SIR resonators, and an L-shaped feed structure is used. In addition, to improve the selectivity of the dual-band filter, a skew-symmetrical $0°$ feeding structure [13] is introduced to achieve extra transmission zeros in the stopband. The stubs are folded to reduce the dual-band bandpass filter size.

According to the resonator analysis, even-mode resonant frequencies of the two resonators are utilized to form the lower passband with the center frequency f_1, and odd-mode resonant frequencies of the two resonators are utilized to form the upper bandpass with the center frequency f_2. The center frequencies (f_1 and f_2) of two passbands can be controlled as follows. We can first determine the center frequency f_2 of the upper passband. It is mainly determined by $L_1 + L_2$, which is nearly quarter-wavelength at f_2. After f_2 is determined, f_1 can be realized by changing L_3, which does not affect
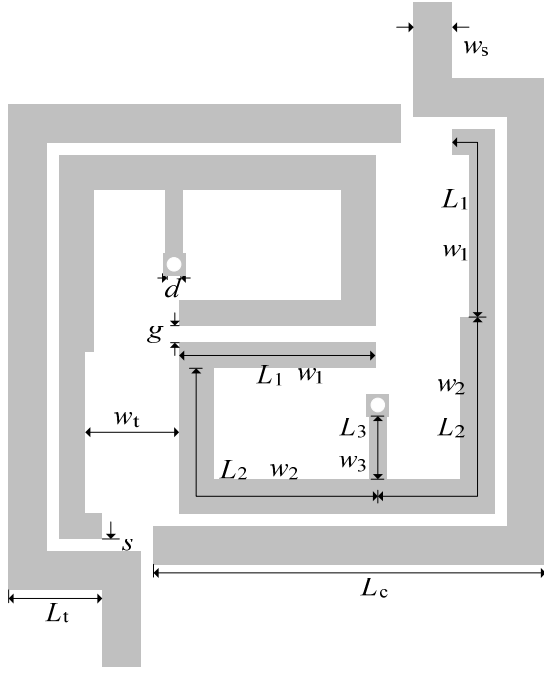
Figure 4. Layout of the designed dual-band bandpass filter.
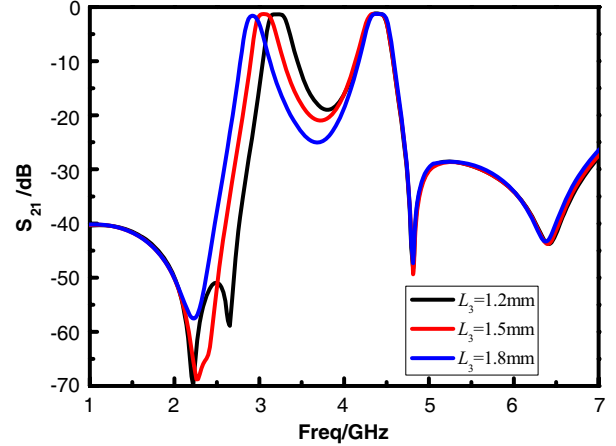
Figure 5. The transmission responses of the proposed dual-band filter with different L_3.

f_2. The length of $L_1 + L_2 + L_3$ is nearly quarter-wavelength at f_1. Thus, the center frequencies of the dual-band bandpass filter can be controlled individually. To demonstrate this, simulations are carried out, and the simulated results are shown in Figure 5. It can be observed that the center frequency f_1 of the lower passband decreases obviously while the center frequency f_2 of the upper passband remain almost unchanged with the increases of the dimension L_3. Thus, it can be concluded that the center frequencies of the two passbands can be controlled individually. The bandwidths of the dual-band passband filter depend on the coupling coefficients (K) and external quality factors (Q_e). The desired values of K and Q_e can be obtained using the synthesis method presented in [14, 15]. K is determined by the coupling among the resonators, e.g., w_t, g, and L_1. Small gaps (w_t and g) and large L_1 result in large K at the two passbands, leading to large bandwidths. Q_e is determined by adjusting the coupling among the L-shaped feed and resonators, e.g., L_t, L_c and s.

4. SIMULATED AND MEASURED RESULTS

To verify the proposed approach, a dual-band bandpass filter is fabricated and measured on a dielectric substrate with a relative dielectric constant of 2.2, thickness of 0.508 mm, and loss tangent of 0.0009. The dimensions are chosen as follows: $L_1 = 5.5$ mm, $w_1 = 0.5$ mm, $L_2 = 8.075$ mm, $w_2 = 0.53$ mm, $L_3 = 1.6$ mm, $w_3 = 0.15$ mm, $s = 0.15$ mm, $g = 0.65$ mm, $L_t = 3.5$ mm, $L_c = 12$ mm, $w_t = 3.65$ mm, $w_s = 1.5$ mm, $d = 0.4$ mm. The size of dual-band filter is about 17.1 mm × 14.65 mm ($0.22\lambda_g \times 0.19\lambda_g$, where λ_g is the guide-wavelength of the first passband frequency). A photograph of the fabricated filter is shown in Figure 6.

The simulation and measurement are accomplished by Ansoft HFSS 13 and E5071C network analyzer, respectively. The simulated and measured transmission responses are illustrated in Figure 7. As observed, a good dual-band filter performance is obtained, and the measured results agree well with the simulated ones. The measured two passbands are centered at 3 and 4.38 GHz with the fractional bandwidths of 8.3 and 4.6%, respectively. The corresponding insertion losses, including the losses from SMA connector, are 1.7 and 1.6 dB, and the return losses within two passbands are better than 20 dB. The attenuation of over 25 dB is observed between two passbands. Five transmission zeros are generated
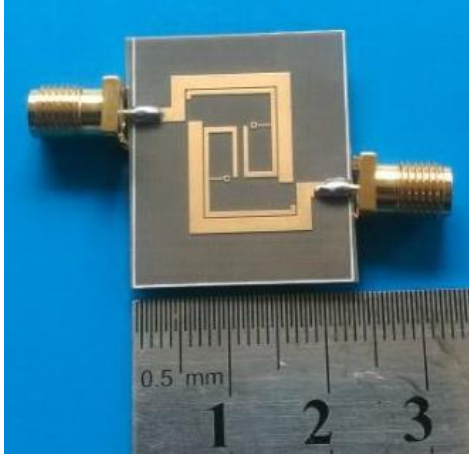
Figure 6. Photograph of the fabricated dual-band filter.
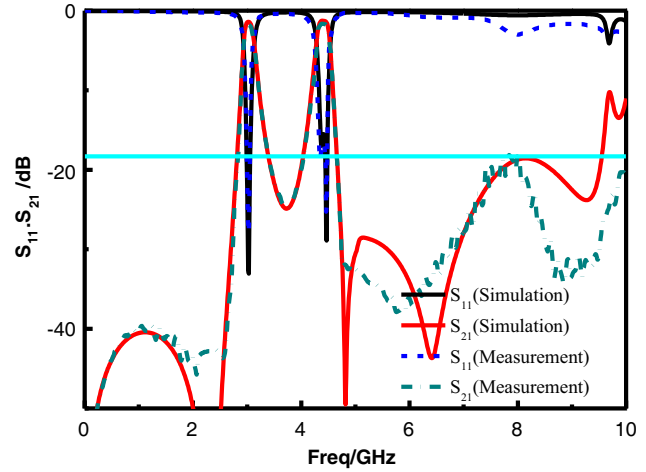
Figure 7. Comparison between the EM simulated and measured results.

at 2.08, 2.53, 4.76, 5.8, and 8.83 GHz. Among them, the first and second transmission zeros improve the low frequency stopband rejection level with more than 40 dB, and the other three transmission zeros improve the high frequency stopband rejection level (the measured rejection is better than 18 dB from 4.8 to 10.1 GHz), featuring high selectivity and wide stopband rejection.

The measured dual-band filter performance is compared with previously reported high performance dual-band filter, as shown in Table 1. The roll-off rate (ROR) in Table 1 is introduced to analyze the selectivity of the proposed dual-band filter, which is defined as:

$$\text{ROR} = \frac{\alpha_{20\,\text{dB}} - \alpha_{3\,\text{dB}}}{f_{20\,\text{dB}} - f_{3\,\text{dB}}} \tag{8}$$

where $\alpha_{20\,\text{dB}}$ is 20 dB attenuation point; $\alpha_{3\,\text{dB}}$ is 3 dB attenuation point; $f_{20\,\text{dB}}$ is 20 dB stopband frequency; $f_{3\,\text{dB}}$ is 3 dB stopband frequency. From Table 1, we can observe that the proposed dual-band filter shows smaller size, lower insertion loss, better band-to-band isolation, wider rejection level, and sharper roll-off, which can effectively characterize the high selectivity of the dual-band passband filter.

Table 1. Comparison between the proposed filter and previous works.

Reference	Size ($\lambda_g \times \lambda_g$)	IL (dB)	FBW (%)	IS (dB)	SW (GHz)	ROR (dB/GHz)
Filter I in [16]	$0.37\lambda_g \times 0.37\lambda_g$	1.34/0.97	9.2/17.1	> 15	1	56.7/48.5/48.5/25
Filter I in [17]	$0.92\lambda_g \times 0.53\lambda_g$	0.79/1.3	18.3/29.1	> 23	3	10/34/42/13
Filter II in [17]	$0.699\lambda_g \times 0.383\lambda_g$	0.76/0.8	25.8/55.7	> 17	1.6	8.1/42.5/26.2/17
[18]	$0.27\lambda_g \times 0.27\lambda_g$	1.05/1.94	21.5/12.2	> 29	1.3	18/13.1/39.5/18.5
[19]	$0.20\lambda_g \times 0.26\lambda_g$	0.21/0.25	8/4.3	> 10	2	51.3/110/42.5/170
[20]	$0.29\lambda_g \times 0.3\lambda_g$	1.16/2.46	7.5/2.83	> 13	NS	170/94.4/130.7/141.6
proposed filter	$0.22\lambda_g \times 0.19\lambda_g$	1.7/1.6	8.3/4.6	> 25	5.3	113.3/56.7/56.7/170

Note: IL, FBW, IS, SW, NS denote insertion loss, 3-dB bandwidth, isolation between two passbands, and more than 18 dB suppression width of the upper stopband, and not shown, respectively.

5. CONCLUSIONS

This letter has presented a dual-band bandpass filter using a dual-mode SIR resonance. The resonator has been analyzed by theory and experiments. The simulated results validate the passband frequencies which can be individually controlled. The size of filter is about $0.22\lambda_g \times 0.19\lambda_g$. The RORs are

113.3/56.7/56.7/170 dB/GHz, which exhibit a high selectivity performance. Five transmission zeros of the upper frequency stopband are achieved at 2.08, 2.53, 4.76, 5.8, and 8.83 GHz, resulting in wide stopband rejection and high selectivity. The measured results are in good agreement with the simulated ones. The compact size, high selectivity, wide stopband rejection, and planar structure make it attractive for future wireless communication systems.

ACKNOWLEDGMENT

REFERENCES

1. Hong, J. S. and M. J. Lancaster, *Microstrip Filters for RF/Microwave Applications*, Wiley, New York, 2001.
2. Tsai, L. C. and C. W. Huse, "Dual-band bandpass filters using equal-length coupled-serial-shunted lines and Z-transform techniques," *IEEE Trans. Microw. Theory Tech.*, Vol. 52, No. 4, 1111–1117, 2004.
3. Chen, F. C., Q. X. Chu, Z. H. Li, and X. H. Wu, "Compact dual-band bandpass filter with controllable bandwidths using stub-loaded multiple-mode resonator," *IET Proc. Microw., Antennas Propag.*, Vol. 6, No. 10, 1172–1178, 2012.
4. Lin, K. C., C. F. Chang, M. C. Wu, and S. J. Chung, "Dual-bandpass filters with serial configuration using LTCC technology," *IEEE Trans. Microw. Theory Tech.*, Vol. 54, No. 6, 2321–2328, 2006.
5. Lee, J. and Y. Lim, "Compact dual-band bandpass filter with good frequency selectivity," *Electron. Lett.*, Vol. 47, No. 25, 1376–1377, 2011.
6. Wei, X. B., Y. Shi, and P. Wang, "Compact dual-band bandpass filter with improved stopband characteristics," *Electron. Lett.*, Vol. 48, No. 12, 704–705, 2012.
7. Zhang, X. Y. and Q. Xue, "Novel dual-mode dual-band bandpass filters using coplanar waveguide fed ring resonators," *IEEE Trans. Microw. Theory Tech.*, Vol. 55, No. 10, 2183–2190, 2007.
8. Chen, C. H. and C. H. Huang, "Highly miniaturized multi-band bandpass filter design based on a stacked spiral resonator structure," *IEEE Trans. Microw. Theory Tech.*, Vol. 60, No. 5, 1278–1286, 2012.
9. Chang, W. S. and C. Y.Chang, "Analytical design of microstrip short-circuit terminated stepped-impedance resonator dual-band filter," *IEEE Trans. Microw. Theory Tech.*, Vol. 59, No. 7, 1730–1739, 2011.
10. Singh, V., V. K. Killamsetty, and B. Mukherjee, "Compact dual-band BPF with wide stopband using stub-loaded spiral stepped-impedance resonator," *Electron. Lett.*, Vol. 52, No. 22, 1860–1862, 2013.
11. Chu, Q. X. and H. Wang, "A compact open-loop filter mixed electric and magnetic coupling," *IEEE Trans. Microw. Theory Tech.*, Vol. 56, No. 2, 431–439, 2008.
12. Zhang, X. Y., J. X. Chen, Q. Xue, and S. M. Li, "Dual-band filter using stub-loaded resonators," *IEEE Microw. Wireless Compon. Lett.*, Vol. 17, No. 8, 583–585, 2007.
13. Tsai, C. M., S. Y. Lee, and C. C. Tsai, "Performance of a planar filter using a 0° feed structure," *IEEE Trans. Microw. Theory Tech.*, Vol. 50, No. 10, 2362–2367, 2002.
14. Chen, C. F., T. Y. Huang, and R. B. Wu, "Design of dual- and triple-passband filters using alternately cascaded multiband resonators," *IEEE Trans. Microw. Theory Tech.*, Vol. 54, No. 9, 3550–3558, 2006.
15. Amari, S., "Direct synthesis of folded symmetric resonator filters with source-load coupling," *IEEE Microw. Wireless Compon. Lett.*, Vol. 11, No. 6, 264–266, 2001.
16. Sun, S. J., L. Lin, B. Wu, K. Deng, and C.-H. Liang, "A novel quad-mode resonator and its application to dual-band bandpass filters," *Progress In Electromagnetics Research Letters*, Vol. 43, 95–104, 2013.

17. Fu, W., Z. M. Li, P. Z. Liu, J. W. Cheng, and X. Qiu, "Modeling and analysis of novel CSRRs-loaded dual-band bandpass SIW filters," *IEEE Trans. Circuits Syst. II, Exp. Briefs*, Vol. 68, No. 7, 2352–2356, 2021.

18. Lahmissi, A. and M. Challal, "Design and analysis of a compact dual-band bandpass filter using V- and W-shaped microstrip open lines," *Microw. Opt. Technol. Lett.*, Vol. 61, 920–925, 2019.

19. Liu, H. W., P. Wen, Y. L. Zhao, B. P. Ren, X. M. Wang, and X. H. Guan, "Dual-band superconducting bandpass filter using quadruple-mode resonator," *IEEE Trans. Appl. Supercond.*, Vol. 24, No. 2, 1–4, 2014.

20. Xu, J., K. D. Xu, M. Zhang, and Q. Chen, "Dual-band bandpass filter using two simple coupled microstrip rings," *Engineering Reports*, Vol. 3, e12288, 2021.